

# Using A Packed-Column Model To Simulate the Performance of A Membrane Absorber

David deMontigny,<sup>†</sup> Ahmed Aboudheir,<sup>†</sup> Paitoon Tontiwachwuthikul,<sup>\*,†</sup> and Amit Chakma<sup>‡</sup>

*International Test Centre for CO<sub>2</sub> Capture, University of Regina, Regina, Saskatchewan S4S 0A2, Canada, and  
Department of Chemical Engineering, University of Waterloo, Waterloo, Ontario N2L 3G1, Canada*

Experimental results from a gas absorption membrane (GAM) system were simulated using a comprehensive mathematical model. Originally, the model was developed to simulate carbon dioxide (CO<sub>2</sub>) absorption into aqueous solutions of monoethanolamine (MEA) in a packed column. The current work has modified the original model and demonstrates that packed-column models can be altered for membrane-based absorption systems, providing that the gas–liquid contacting mechanism is considered. The experimental data was generated using three GAM modules connected in series that contained microporous hollow-fiber poly(tetrafluoroethylene) (PTFE) membranes. Simulation results showed that the model predicted the performance of the GAM system with reasonable accuracy. The average absolute deviation (ADD) of the model was 1.9%. This work has demonstrated that packed-column models can be modified with relative ease to simulate the performance of GAM systems.

## 1. Introduction

The capture of CO<sub>2</sub> from industrial flue gases has traditionally been carried out in large absorption plants that are subject to liquid channeling, flooding, entrainment, and foaming problems. Emerging gas absorption membrane (GAM) technology has the potential to replace packed columns with smaller, cheaper membrane modules that avoid these problems.<sup>1</sup> Mass transfer in GAM systems occurs after the gas has diffused through a microporous membrane that separates the gas and liquid phases. The membrane provides a contact area for the mass transfer to occur, much like the packing in a packed column. This is depicted in Figure 1 for CO<sub>2</sub> absorption in a GAM system. Kumar et al.<sup>2</sup> identified the advantages of this type of arrangement, which include independent liquid and gas flow, a high surface area-to-volume ratio, and linear scale-up. On the negative side, Dindore et al.<sup>3</sup> noted that the membrane adds an additional level of resistance to mass transfer. This resistance can be significant if the membrane is wetted by the absorption solution.

During the past twenty years, a great deal of research has been conducted to evaluate the performance of GAM systems, both experimentally and mathematically. The idea to use microporous membranes as contactors in CO<sub>2</sub> absorption processes was first proposed by Qi and Cussler.<sup>4,5</sup> Their initial work showed that hollow-fiber membranes could be used in absorption applications. They concluded that membrane modules have an advantage over packed towers because of their large surface area-to-volume ratio and independent liquid and gas flow rates; however, the membrane adds a new element of resistance to mass transfer. Work by Karoor and Sirkar<sup>6</sup> studied acid gas absorption into water using GAM systems containing polypropylene (PP) membranes. They found that, when the membranes became wetted, the resistance to mass transfer was higher. A mathematical model developed to simulate their experimental results produced values that were in good agreement with the

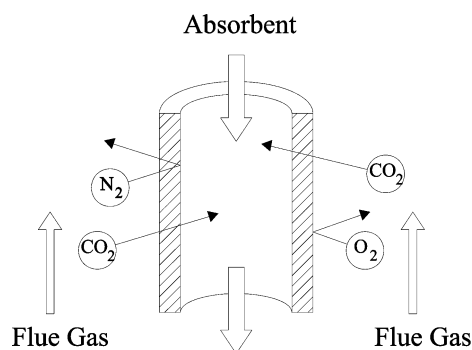


**Figure 1.** Mass transfer in a microporous GAM system.

experimental data. Kim and Yang<sup>7</sup> used a GAM system containing poly(tetrafluoroethylene) (PTFE) membranes to absorb CO<sub>2</sub> into various amine solutions. Results from their mathematical model were comparable to the experimental values. Lee et al.<sup>8</sup> conducted a comprehensive numerical analysis on GAM systems. Numerical solutions were employed to solve the nonlinear partial-differential equations. The model worked, but they lacked the experimental data to evaluate the accuracy of the simulations. Work by Kumar et al.<sup>2</sup> tested amino acid salt solutions for CO<sub>2</sub> absorption in GAM systems containing PP membranes. The work addressed the wetting problem that is common with amines and polyolefin membranes. They developed a numerical model for their system that predicted experimental values within 25%, given a wide range of operating conditions. Hoff et al.<sup>9</sup> studied the absorption of CO<sub>2</sub> into monoethanolamine (MEA) and methyldiethanolamine (MDEA) solutions in a GAM system containing PTFE membranes. Their comprehensive model predicted the experimental results with a good degree of accuracy. Until very recently, no reports of GAM experiments using two or more modules in series had appeared in the literature. Dindore et al.<sup>10</sup> investigated a cross-flow GAM system that operated with up to four modules in series. Acid gases were absorbed into solutions of potassium carbonate. A detailed mathematical model based on first principles was able to accurately predict the experimental data generated by the GAM system.

\* To whom correspondence should be addressed. Tel.: (306) 585-4160. Fax: (306) 585-4855. E-mail: paitoon@uregina.ca.

<sup>†</sup> University of Regina.

<sup>‡</sup> University of Waterloo.

## B

**Table 1. Membrane and Membrane Module Characteristics**

Description of 2-mm PTFE Hollow-Fiber Membranes	
fiber outer diameter (mm)	2.0
fiber inside diameter (mm)	1.0
wall thickness (mm)	0.5
membrane porosity (%)	50
membrane length (m)	0.122
Description of Membrane Modules	
fibers per module	57
outside specific area (m <sup>2</sup> /m <sup>3</sup> )	581.6
inside specific area (m <sup>2</sup> /m <sup>3</sup> )	290.8
module void fraction (%)	70.9

In the current work, three GAM modules containing PTFE membranes were connected in series to absorb CO<sub>2</sub> into aqueous monoethanolamine solutions. A study by Falk-Pederson and Dannström<sup>11</sup> suggested that PTFE is the only suitable membrane for use with alkanolamines. System performance was modeled using a comprehensive mathematical model that was originally developed for packed columns. By properly accounting for the gas–liquid contact area, the simulation results were in good agreement with the experimental data.

## 2. Experimental Work

A total of 10 experiments were done to assess the performance of the GAM system. Three identical membrane modules were built and connected in series to form the GAM system. Each module contained 57 microporous PTFE hollow-fiber membranes. Table 1 lists the characteristics of the membranes and the modules. Aqueous solutions of MEA were used to absorb CO<sub>2</sub> from a simulated flue gas stream containing CO<sub>2</sub> and air. A detailed description of the GAM system design and the experimental procedures has been provided elsewhere,<sup>12</sup> and only brief details will be provided here.

Membrane modules were built using acrylic tubing that had an inside diameter of 28 mm and a 6 mm wall thickness. Each module was roughly 0.25 m long with gas, liquid, and temperature sampling points located along its length. The system was operated under a countercurrent flow regime for optimum performance. The simulated flue gas stream entered at the top of the module on the shell-side and flowed down, while lean liquid solution entered at the bottom of the system and flowed upward through the hollow-fiber lumen. Previous work by deMontigny et al.<sup>13</sup> has shown that the mass transfer performance of GAM systems is better when the liquid flows through the lumen. Figure 2 shows a schematic of the experimental

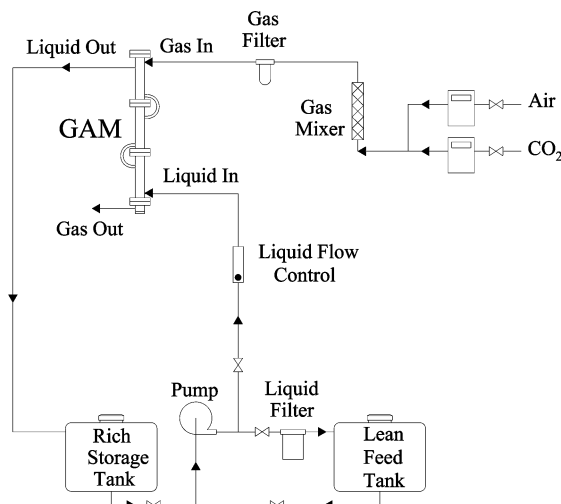


**Figure 2.** Schematic of experimental CO<sub>2</sub> absorption apparatus.

**Table 2. Experimental Operating Conditions**

operating condition	range
inert gas flow rate (kmol/(m <sup>2</sup> ·h))	31.6
liquid flow rate (m <sup>3</sup> /m <sup>2</sup> ·h)	73.3–173.2
MEA concentration (kmol/m <sup>3</sup> )	2.0
CO <sub>2</sub> feed concentration (%)	9.5–15.2
feed solution CO <sub>2</sub> loading (kmol/kmol)	0.28

apparatus. During steady-state conditions, the concentration of CO<sub>2</sub> in the gas phase was measured along the length of the GAM system using the infrared gas analyzer. Gas and liquid temperatures inside the contactor were measured and liquid samples were collected and analyzed for their CO<sub>2</sub> loading. Table 2 lists the experimental operating conditions.

## 3. Model Development

The goal of the modeling component in this work was to show that mathematical models originally developed for packed columns can be used to simulate the performance of GAM systems. Providing that the contact between gas and liquid phases is properly accounted for, absorption models should work regardless of whether the contacting medium was packing or a membrane. Aboudheir et al.<sup>14</sup> developed a rigorous computer program for CO<sub>2</sub> absorption with MEA solutions in randomly packed columns. The model contained three main components: (1) a material and energy balance model developed by Pandya;<sup>15</sup> (2) a vapor–liquid equilibrium (VLE) model and termolecular-kinetics model developed by Aboudheir et al.;<sup>14</sup> and (3) physical properties published in the literature. Pandya's material and energy balance model was the first work on design techniques for gas absorption with chemical reaction in adiabatic packed towers. The model considers heat effects from absorption, solvent evaporation, and condensation, plus it accounts for the chemical reaction in the liquid phase as well as the heat and mass transfer resistances in both phases. Aboudheir et al.<sup>14</sup> used Pandya's methodology, in combination with their own VLE and termolecular-kinetics models, to simulate the CO<sub>2</sub> absorption process in packed-bed columns. The model was written in FORTRAN 90 and works very well for absorption columns packed with random packing.<sup>14,16</sup> The current work has expanded this model to simulate the absorption performance of GAM systems.

Pandya<sup>15</sup> made the following assumptions in order to write the main equations for the mass and energy balances in his model: (1) the reaction is fast and occurs in the liquid film such that the bulk liquid is in equilibrium; (2) liquid-phase heat transfer resistance is small when compared to that in the gas phase; (3) mass transfer resistance for water in the liquid phase is negligible; (4) the interfacial area for heat and mass transfer is the same; and (5) only CO<sub>2</sub> and water vapor can cross the gas–liquid interface. The system is also assumed to operate under steady-state conditions. On the basis of these assumptions, the main equations required for the mass and energy balances were written. For the concentration gradients of the gas species, Pandya<sup>15</sup> wrote the following:

$$\frac{dY_A}{dZ} = \frac{-k_{A,G}aP(y_{A,G} - y_{A,i})}{G_B} \quad (1)$$

$$\frac{dY_S}{dZ} = \frac{-k_{S,G}aP(y_{S,G} - y_{S,i})}{G_B} \quad (2)$$

Temperature gradients were written for both the gas and liquid phases:

$$\frac{dT_G}{dZ} = \frac{-h_G a(T_G - T_L)}{G_B(C_{PB} + Y_A C_{PA} + Y_S C_{PS})} \quad (3)$$

$$\frac{dT_L}{dZ} = \frac{1}{L_M C_{PL}} \left( G_B(C_{PB} + Y_A C_{PA} + Y_S C_{PS}) \frac{dT_G}{dZ} + G_B(C_{PS}(T_G - T_0) + \lambda_S) \frac{dY_S}{dZ} + G_B(C_{PA}(T_G - T_0) - \Delta H_R(T_0, P)) \frac{dY_A}{dZ} \right) \quad (4)$$

When it comes to modeling absorption processes, usually the inlet gas and liquid conditions are known, and the outlet conditions are unknown. Aboudheir solved this two-point boundary value problem in his model using the shooting method. By initially assuming that the temperature and moisture content of the outlet gas is in equilibrium with the inlet liquid, the outlet liquid conditions can be determined by applying mass and energy balances across the absorber. The shooting-method solution progresses upward along the column, computing profiles for the temperature and concentration until the specified CO<sub>2</sub> outlet concentration is achieved. If the calculated conditions at the top of the column do not converge with the initially assumed values, new outlet gas conditions are assumed and the procedure is repeated. This procedure is outlined in Figure 3, which shows a simplified flowchart for the FORTRAN 90 program that solves the system of equations (eqs 1–5). The parameters demanded by the model for each absorption case are obtained from available experimental measurements or correlations. These parameters are programmed into subroutines that are called by the main program at each operating condition. More details on the original model can be found in Aboudheir et al.<sup>16</sup>

**3.1. Correlations Used in the GAM Model.** To adapt Aboudheir's model for GAM systems, correlations for the effective surface area ( $A_e$ ), the gas-phase mass transfer coefficient ( $k_G$ ), and the liquid-phase mass transfer coefficient ( $k_L$ ) had to be changed. According to Geankoplis,<sup>17</sup> mass transfer coefficients that are obtained from a variety of fluid systems, geometries, and operating parameters can be correlated using dimensionless numbers. This allows for performance comparisons between different systems. These correlations typically result in a general equation of the form

$$Sh = f(Re, Sc) \quad (5)$$

where  $Sh$  is the Sherwood number,  $Re$  is the Reynolds number, and  $Sc$  is the Schmidt number. By selecting appropriate correlations to calculate the gas- and liquid-phase mass transfer coefficients in a GAM system, it was possible to modify Aboudheir's packed-column model to simulate the performance of the GAM system used in this study. Table 3 lists a variety of mass transfer correlations published in the literature for CO<sub>2</sub> removal in GAM systems. There are numerous mass transfer correlations published in the literature, because GAM systems come in a variety of configurations:

- Flow in the fiber lumen: liquid or gas;
- System orientation: cocurrent or countercurrent;
- Shell-side flow: parallel to the fibers or perpendicular to the fibers;
- Hollow-fiber packing density and arrangement.

In this work, the liquid-phase flowed in the hollow-fiber lumen. Correlations proposed by Nii and Takeuchi<sup>18</sup> were selected because they also tested microporous PTFE membranes with alkanolamines for CO<sub>2</sub> capture. In the simulation work of

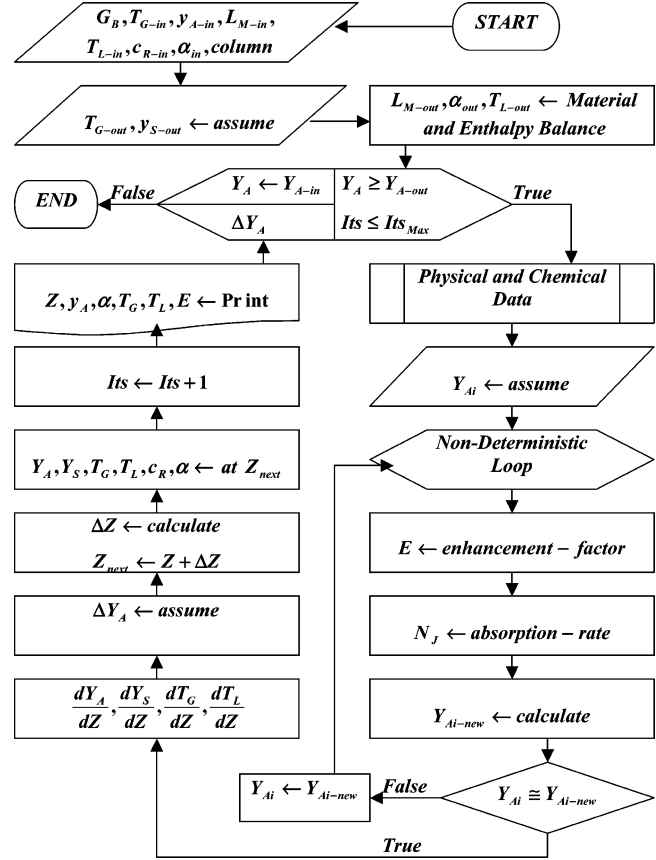


Figure 3. Flowchart for the simulation model.

Table 3. Mass Transfer Correlations for CO<sub>2</sub> Removal in GAM Systems

source	correlations	lumen side
Nii and Takeuchi <sup>18</sup>	$Sh_G = 0.41(1/n)(d_s/d_o)^{2.0}(d_w/d_l)^{0.25}Re^{0.33}Sc^{0.33}$ $Sh_L = 1.62((d_i/Z)ReSc)^{0.33}$	liquid
Rangwala <sup>19</sup>	$Sh_G = 0.0025(P/P_{BM})Re^{0.83}Sc^{0.44}$ $Sh_L = 1.62Gz^{0.33} = 1.62(d_i^2 u_L / D_l Z)^{0.33}$	liquid
Bhaumik et al. <sup>20</sup>	$Sh_L = 0.57Re^{0.31}Sc^{0.33}$	gas
Ferreira et al. <sup>21</sup>	$Sh_L = 0.39Re^{0.59}Sc^{0.33}$	gas
Li and Teo <sup>22</sup>	$Sh_L = 1.164(d_w/ZRe)^{0.967}Sc^{0.33}$	gas
Feron and Jansen <sup>1</sup>	$Sh_G = 0.9Re^{0.5}Sc^{0.33}$ $Sh_L = ((4^3 + 1.8^3 Re Sc d_i)/Z)^{0.33}$	liquid

Nii and Takeuchi, they modified an equation proposed by Takeuchi et al.<sup>23</sup> to calculate the  $k_G$ , and they used the L ev eque<sup>24</sup> equation to calculate the  $k_L$ . The expanded forms of these equations are given below:

$$k_G = 0.41 \frac{D_A}{d_e RT} \frac{1}{n} \left( \frac{d_s}{d_o} \right)^{2.0} \left( \frac{d_e}{L} \right)^{0.25} \left( \frac{d_e u_G}{v_G} \right)^{0.33} \left( \frac{v_G}{D_A} \right)^{0.33} \quad (6)$$

$$k_L = 1.62 \frac{D_A}{d_i} \left( \frac{d_i}{L} \right)^{0.33} \left( \frac{d_i u_L}{v_L} \right)^{0.33} \left( \frac{v_L}{D_A} \right)^{0.33} \quad (7)$$

When the liquid phase flows through the fiber lumen, it can be assumed that  $A_e$  equals the total surface area, such that

$$A_e = A_T \quad (8)$$

**3.2. Adapting the Correlations.** When the correlations presented by Nii and Takeuchi<sup>18</sup> were used as presented, the model predicted the experimental results with a high degree of accuracy. The average absolute deviation was 2.66% when using the original equation. This can be seen in Figure 4, where a

D

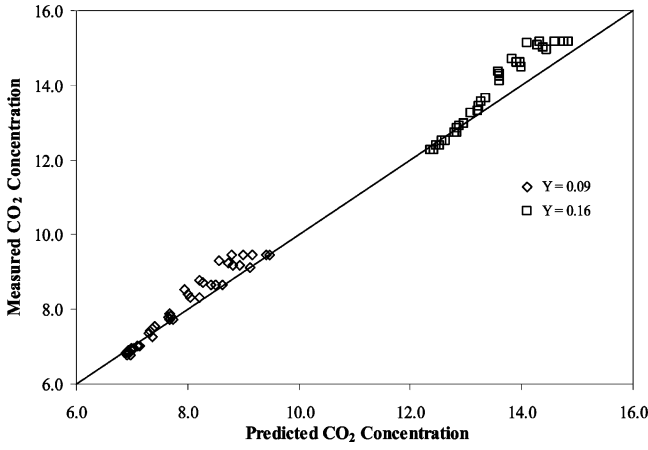


**Figure 4.** Parity plot for the model using the original correlations of Nii and Takeuchi.

parity plot of the predicted results and the experimental results is shown. While these results are good, an effort was made to improve the accuracy by conducting a nonlinear regression analysis on one of the correlations in the model. Since the effective area is fixed in the GAM system and the liquid flowed through the fiber lumen, eq 7 was chosen for the regression in an attempt to identify new  $X_1$  and  $X_2$  coefficients:

$$k_L \text{ correlation: } k_L = X_1 \frac{D_A(d_i)}{d_i(L)}^{X_2} \left( \frac{d_i u_L}{\nu_L} \right)^{X_2} \left( \frac{\nu_L}{D_A} \right)^{X_2} \quad (9)$$

The nonlinear regression program was run to minimize the following error function,

$$F(I) = k_L(I)|_{\text{fitted}} - \left( X(1) \frac{D_A(I)}{d_i(I)} \left( \frac{d_i(I)}{L(I)} ReSc \right)^{X(2)} \right) \quad (10)$$

where  $X(1)$  and  $X(2)$  are the coefficients in the Nii and Takeuchi liquid-phase mass-transfer-coefficient correlation.

#### 4. Results, Analysis, and Discussion

A total of 10 different runs were conducted using the GAM system. Two sets of experiments were conducted that measured the effect of liquid flow rate on mass transfer rates. One set of experiments was conducted with a gas-phase  $\text{CO}_2$  feed concentration of roughly 9.5%, and the second set of experiments

was conducted at a gas-phase  $\text{CO}_2$  feed concentration of roughly 15.2%. The experimental results are listed in Table 4 for all 10 experiments. Inlet and outlet temperatures are given for both the gas and liquid phases. Note that the temperature values did not change a great deal over the length of the GAM system. This can be attributed to the relatively small modules. Larger temperature differences are seen in taller packed columns. The effect of having a smaller reactor is also seen in the  $\text{CO}_2$  removal rates, which range from 13 to 20%. A larger reactor would display a more prominent temperature profile and capture the bulk of the  $\text{CO}_2$  gas. This is not to say that a GAM system cannot achieve high levels of performance. In fact, GAM systems have been shown to perform better than packed columns.<sup>12</sup>

The simulation results obtained using the modified Nii and Takeuchi  $k_L$  correlation are shown in the parity plot in Figure 5. A slight improvement in the results is observed when compared to the simulation that used the original Nii and Takeuchi  $k_L$  correlation. The original equation produced results that had an average absolute deviation of 2.66%, while the modified equation had an average absolute deviation of 1.91%. The new liquid-phase mass-transfer-coefficient correlation is given below:

Original Nii and Takeuchi correlation:

$$k_L = 1.62 \frac{D_A(d_i)}{d_i(L)}^{0.33} \left( \frac{d_i u_L}{\nu_L} \right)^{0.33} \left( \frac{\nu_L}{D_A} \right)^{0.33} \quad (7)$$

Modified Nii and Takeuchi correlation:

$$k_L = 2.07 \frac{D_A(d_i)}{d_i(L)}^{0.33} \left( \frac{d_i u_L}{\nu_L} \right)^{0.33} \left( \frac{\nu_L}{D_A} \right)^{0.33} \quad (11)$$

The degree of improvement between the original and modified Nii and Takeuchi correlations is small and does not have a huge impact on the results. The main focus of this work was to modify an existing packed-column model so that it could successfully simulate a GAM system. This was achieved with the original Nii and Takeuchi correlation. However, since it did not require much further work to complete a regression analysis, the modified correlation was developed.

In comparing the simulation results from both sets of experimental data, it was noticed that the model tended to produce more accurate results at the bottom of the GAM system where the gas-phase  $\text{CO}_2$  concentration was low. This is evident

**Table 4. Experimental  $\text{CO}_2$  Absorption Data Using the GAM System**

description	run 1	run 2	run 3	run 4	run 5	run 6	run 7	run 8	run 9	run 10
inert gas flow (kmol/(m <sup>2</sup> ·h))	31.6	31.6	31.6	31.6	31.6	31.6	31.6	31.6	31.6	31.6
liquid flow rate (m <sup>3</sup> /(m <sup>2</sup> ·h))	73.5	92.5	115.0	146.1	173.2	73.3	92.2	115.0	145.6	173.0
MEA concentration (kmol/m <sup>3</sup> )	2.0	2.0	2.0	2.0	2.0	2.0	2.0	2.0	2.0	2.0
inlet $\text{CO}_2$ loading (kmol/kmol)	0.278	0.278	0.278	0.278	0.278	0.275	0.275	0.275	0.275	0.275
outlet $\text{CO}_2$ loading (kmol/kmol)	0.360	0.345	0.332	0.322	0.316	0.371	0.354	0.343	0.330	0.323
liquid inlet temp. (°C)	23.5	23.2	23.0	22.7	22.6	22.1	21.4	21.0	20.4	19.8
liquid outlet temp. (°C)	23.9	23.7	23.3	23.1	22.9	22.9	22.2	22.1	21.5	21.0
gas inlet temp. (°C)	22.0	21.9	21.8	21.7	21.6	21.2	20.8	21.2	20.9	20.5
gas outlet temp. (°C)	22.1	21.9	21.8	21.6	21.4	21.4	20.7	21.1	20.5	20.4
$\text{CO}_2$ removal (%)	19.1	18.6	19.3	18.8	19.6	13.0	13.9	14.4	14.9	15.0
mass balance error (%)	-3.6	-1.9	-4.0	-3.5	-2.2	-1.4	-2.1	-1.1	-1.8	-2.4
gas-phase $\text{CO}_2$ concentration (%)										
(# 7) 0.367 <sup>a</sup>	9.47	9.47	9.47	9.47	9.47	15.18	15.18	15.18	15.18	15.18
(# 6) 0.306 <sup>a</sup>	9.29	9.23	9.18	9.18	9.12	15.12	15.12	15.06	15.01	14.95
(# 5) 0.244 <sup>a</sup>	8.77	8.71	8.65	8.65	8.65	14.72	14.66	14.60	14.60	14.48
(# 4) 0.183 <sup>a</sup>	8.54	8.42	8.42	8.30	8.30	14.37	14.37	14.31	14.25	14.13
(# 3) 0.122 <sup>a</sup>	7.89	7.84	7.78	7.72	7.72	13.67	13.61	13.55	13.43	13.32
(# 2) 0.061 <sup>a</sup>	7.54	7.49	7.43	7.37	7.25	13.26	13.20	12.97	12.91	12.85
(# 1) 0.000 <sup>a</sup>	7.02	6.96	6.90	6.84	6.79	12.73	12.62	12.50	12.38	12.27

<sup>a</sup> Indicates sample point number and height from bottom (m).

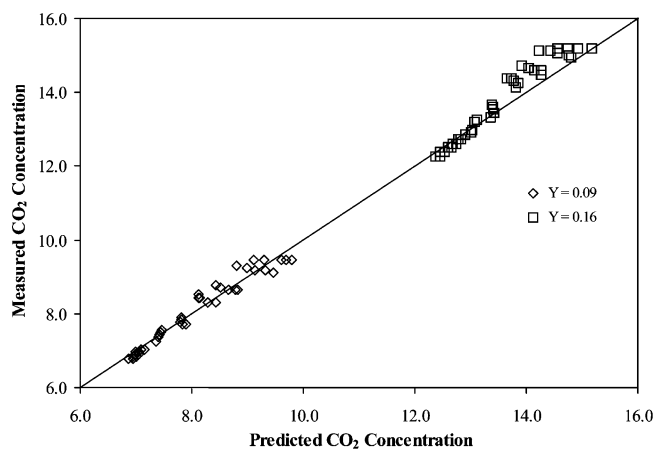


Figure 5. Parity plot for the model using the modified  $k_L$  correlation.

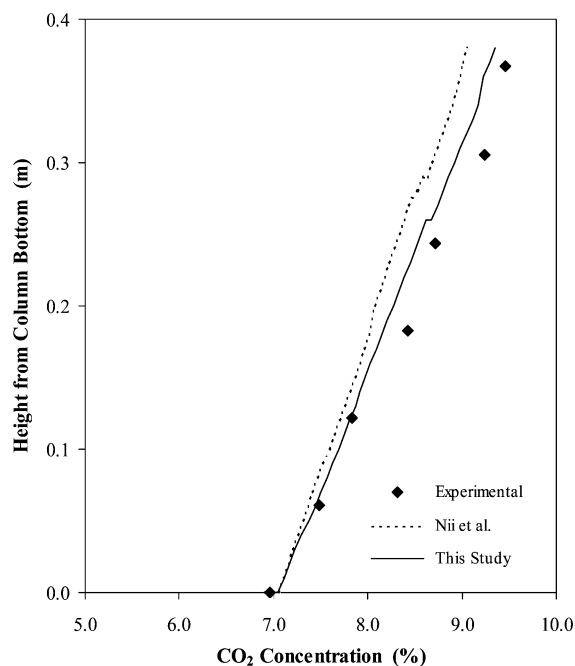


Figure 6. Comparing the experimental and simulation results for Run 2.

in both Figures 4 and 5 for the lower end of the two experimental data sets. The more accurate data points were collected from the middle of the GAM system downward, toward the gas outlet and liquid inlet. The inaccurate data points represent the gas inlet and liquid outlet, where the solution  $\text{CO}_2$  loading is high. At the moment, there is no concrete explanation for this behavior. The termolecular-kinetics model developed by Aboudheir et al.<sup>25</sup> was for highly concentrated and highly loaded MEA solutions. Since the  $\text{CO}_2$  loading was in the range of 0.30 kmol/kmol, this should not have been a problem. It is possible that the low solution concentration of 2.0 kmol/m<sup>3</sup> was a factor, but one would expect this to affect the simulation along the length of the entire GAM system and not just half of the system.

A second trend that was noticed in the simulation results had to do with the effect of liquid flow rate. Five different liquid flow rates were evaluated for each set of experiments. As the liquid flow rate increased, the simulation results shifted to the right and, therefore, tended to improve. For both the  $Y = 0.09$  and  $Y = 0.16$  data sets, the runs with the higher liquid flow rates had the most accurate simulation results. With this in mind, the validity of the model is reduced when the flow rate is low, especially when it is  $<100 \text{ m}^3/(\text{m}^2\cdot\text{h})$ .

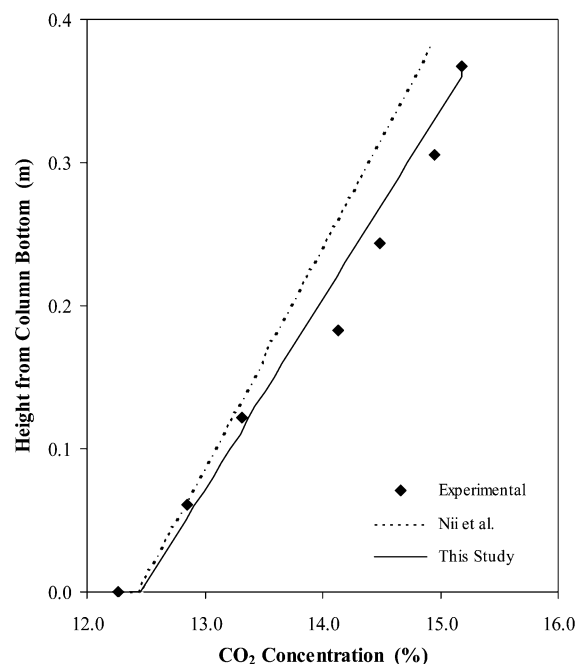


Figure 7. Comparing the experimental and simulation results for Run 10.

Overall, the simulation results for both the original and modified correlations are in good agreement with the experimental data. While the original equation worked well and had a very low average absolute deviation, a small improvement has been made to the liquid-phase mass-transfer-coefficient correlation to better fit the experimental data. Sample plots are shown for the simulation results from two of the GAM experiments. Figure 6 shows the results for a run from the first set of experiments when the gas-phase  $\text{CO}_2$  feed concentration was low, and Figure 7 shows the results for a run from the second set of experiments when the gas-phase  $\text{CO}_2$  feed concentration was high. Both of these figures show that the model was able to predict the experimental data with a high degree of accuracy. These figures also show the improvement gained over the original Nii and Takeuchi model when using the modified  $k_L$  correlation.

## 5. Conclusions

New GAM technology has been tested in a bench-scale  $\text{CO}_2$  absorption plant. PTFE membranes were used inside the contactor, which was operated using aqueous MEA solutions. Three modules were connected in series and operated in a countercurrent flow regime. The system performed well and encountered no operational challenges. A mathematical model that was originally developed for packed columns by Aboudheir et al.<sup>14</sup> was expanded to simulate the GAM system. Correlations proposed by Nii and Takeuchi<sup>18</sup> for the  $k_G$  and  $k_L$  were used in the model and produced satisfactory results. A new correlation for the  $k_L$  has been proposed which offers slightly better results. The model suffered a slight loss in accuracy when the liquid flow rate fell below  $100 \text{ m}^3/(\text{m}^2\cdot\text{h})$ . This work has shown that it is possible to customize existing absorption models for GAM systems by properly accounting for the gas–liquid contacting mechanism.

## Acknowledgment

Financial support from the Natural Sciences and Engineering Research Council, IODE Canada, and The City of Regina is

gratefully acknowledged. We also thank Mitsubishi Rayon Ltd. in Japan for donating the polypropylene membranes.

## Nomenclature

$a$  = interfacial area per unit of packing ( $\text{m}^2/\text{m}^3$ )  
 $A_e$  = effective surface area ( $\text{m}^2/\text{m}^3$ )  
 $C_{P,j}$  = heat capacity of component  $j$  ( $\text{kcal}/(\text{kmol}\cdot\text{K})$ )  
 $G_B$  = total molar gas flow rate ( $\text{kmol}/(\text{m}^2\cdot\text{hr})$ )  
 $h_G$  = heat transfer coefficient ( $\text{kcal}/(\text{m}^2\cdot\text{hr}\cdot\text{K})$ )  
 $\Delta H_R$  = heat of chemical reaction between the absorbed gas and the amine ( $\text{kcal}/\text{kmol}$ )  
 $k_G$  = gas-phase mass transfer coefficient ( $\text{kmol}/(\text{m}^2\cdot\text{s}\cdot\text{kPa})$ )  
 $k_{j,G}$  = gas-phase mass transfer coefficient for component  $j$  ( $\text{kmol}/(\text{m}^2\cdot\text{s}\cdot\text{kPa})$ )  
 $k_L$  = liquid-gas-phase mass transfer coefficient for component  $j$  ( $\text{kmol}/(\text{m}^2\cdot\text{s}\cdot\text{kPa})$ )  
 $L_M$  = liquid mass velocity, ( $\text{kmol}/(\text{m}^2\cdot\text{hr})$ )  
 $P$  = total system pressure (kPa)  
 $Re$  = Reynolds number  
 $Sc$  = Schmidt number  
 $Sh$  = Sherwood number  
 $T$  = temperature (K)  
 $Y_{j,G}$  = mole ratio of component  $j$  in the bulk gas-phase  
 $y_{j,i}$  = mole fraction of component  $j$  at the membrane–liquid interface  
 $y_j$  = mole fraction of component  $j$   
 $Y_j$  = mole ratio of component  $j$  in the bulk gas (kmol/kmol)  
 $Z$  = height of packed column or effective membrane length (m)

## Subscripts

A = component A, solute gas  
 B = component B, the nonsoluble carrier gas  
 G = gas  
 i = interface  
 L = liquid  
 o = base for enthalpy or bulk liquid concentration  
 P = pressure  
 S = volatile solvent

## Literature Cited

- (1) Feron, P. H. M.; Jansen, A. E. CO<sub>2</sub> Separation with Polyolefin Membrane Contactors and Dedicated Absorption Liquids: Performances and Prospects. *Sep. Purif. Technol.* **2002**, *27*, 231.
- (2) Kumar, P. S.; Hogendoorn, J. A.; Feron, P. H. M.; Versteeg, G. F. New Absorption Liquids for the Removal of CO<sub>2</sub> from Dilute Gas Streams Using Membrane Contactors. *Chem. Eng. Sci.* **2002**, *57*, 1639.
- (3) Dindore, V. Y.; Brilman, D. W. F.; Geuzebroek, F. H.; Versteeg, G. F. Membrane–Solvent Selection for CO<sub>2</sub> Removal Using Membrane Gas–Liquid Contactors. *Sep. Purif. Technol.* **2004**, *40*, 133.
- (4) Qi, Z.; Cussler, E. L. Microporous Hollow Fibers for Gas Absorption. I. Mass Transfer in the Liquid. *J. Membr. Sci.* **1985**, *23*, 321.
- (5) Qi, Z.; Cussler, E. L. Microporous Hollow Fibers for Gas Absorption. II. Mass Transfer Across the Membrane. *J. Membr. Sci.* **1985**, *23*, 333.
- (6) Karoor, S.; Sirkar, K. K. Gas Absorption Studies in Microporous Hollow Fiber Membrane Modules. *Ind. Eng. Chem. Res.* **1993**, *32*, 674.
- (7) Kim, Y.; Yang, S. Absorption of Carbon Dioxide Through Hollow Fiber Membranes Using Various Aqueous Absorbents. *Sep. Purif. Technol.* **2000**, *21*, 101.
- (8) Lee, Y.; Noble, R. D.; Yeom, B.; Park, Y.; Lee, K. Analysis of CO<sub>2</sub> Removal by Hollow Fiber Membrane Contactors. *J. Membr. Sci.* **2001**, *194*, 57.
- (9) Hoff, K. A.; Juliussen, O.; Falk-Pedersen, O.; Svendsen, H. F. Modeling and Experimental Study of Carbon Dioxide Absorption in Aqueous Alkanolamine Solutions Using a Membrane Contactor. *Ind. Eng. Chem. Res.* **2004**, *43*, 4908.
- (10) Dindore, V. Y.; Brilman, D. W. F.; Versteeg, G. F. Modeling of Cross-flow Membrane Contactors: Mass Transfer with Chemical Reactions. *J. Membr. Sci.* **2005**, *255*, 275.
- (11) Falk-Pedersen, O.; Dannström, H. Separation of Carbon Dioxide from Offshore Gas Turbine Exhaust. *Energy Convers. Manage.* **1997**, *38*, S81.
- (12) deMontigny, D.; Tontiwachwuthikul, P.; Chakma, A. Comparing the Absorption Performance of Packed Columns and Membrane Contactors. *Ind. Eng. Chem. Res.* **2005**, *44*, 5726.
- (13) deMontigny, D.; Tontiwachwuthikul, P.; Chakma, A. Using Polypropylene and Poly(tetrafluoroethylene) Membranes in a Membrane Contactor for CO<sub>2</sub> Absorption. *J. Membr. Sci.* In press.
- (14) Aboudheir, A.; Tontiwachwuthikul, P.; Wilson, M.; Idem, R. Applications of New Absorption Kinetics and Vapor/Liquid Equilibrium Models to Simulation of a Pilot Plant for Carbon Dioxide Absorption into High CO<sub>2</sub>-Loaded, Concentrated Aqueous Monoethanolamine Solutions. *Sep. Purif. Technol.* Submitted for publication March 2005.
- (15) Pandya, J. D. Adiabatic Gas Absorption and Stripping with Chemical Reaction in Packed Towers. *Chem. Eng. Commun.* **1983**, *19*, 343.
- (16) Aboudheir, A.; Tontiwachwuthikul, P.; Idem, R. A Rigorous Model for Predicting the Behavior of CO<sub>2</sub> Absorption into AMP in Packed-Bed Absorption Columns. *Ind. Eng. Chem. Res.* **2005**, *44*, published online Nov 25, <http://dx.doi.org/10.1021/ie050570d>.
- (17) Geankoplis, C. J. *Transport Processes and Unit Operations*, 3rd ed.; Prentice Hall: Upper Saddle River, NJ, 1993.
- (18) Nii, S.; Takeuchi, H. Removal of CO<sub>2</sub> and/or SO<sub>2</sub> from Gas Streams by a Membrane Absorption Method. *Gas Sep. Purif.* **1994**, *8*, 107.
- (19) Rangwala, H. A. Absorption of Carbon Dioxide into Aqueous Solutions Using Hollow Fiber Membrane Contactors. *J. Membr. Sci.* **1996**, *112*, 229.
- (20) Bhaumik, D.; Majumdar, S.; Sirkar, K. K. Absorption of CO<sub>2</sub> in a Transverse Flow Hollow Fiber Membrane Module Having a Few Wraps of the Fiber Mat. *J. Membr. Sci.* **1998**, *138*, 77.
- (21) Ferreira, B. S.; Fernandes, H. L.; Reis, A.; Mateus, M. Microporous Hollow Fibres for Carbon Dioxide Absorption: Mass Transfer Model Fitting and the Supplying of Carbon Dioxide to Microalgal Cultures. *J. Chem. Technol. Biotechnol.* **1998**, *71*, 61.
- (22) Li, K.; Teo, W. K. Use of Permeation and Absorption Methods for CO<sub>2</sub> Removal in Hollow Fibre Membrane Modules. *Sep. Purif. Technol.* **1998**, *13*, 79.
- (23) Takeuchi, H.; Takahashi, K.; Nakano, M. Mass Transfer in Single Oil-Containing Microporous Hollow Fiber Contactors. *Ind. Eng. Chem. Res.* **1990**, *29*, 1471.
- (24) Lévêque, J. A. Les Lois de la Transmission de Chaleur par Convection. *Ann. Mines* **1928**, *13*, 201.
- (25) Aboudheir, A.; Tontiwachwuthikul, P.; Chakma, A.; Idem, R. Kinetics of the Reactive Absorption of Carbon Dioxide in High CO<sub>2</sub>-loaded, Concentrated Aqueous Monoethanolamine Solutions. *Chem. Eng. Sci.* **2003**, *58*, 5195.

Received for review May 15, 2005

Revised manuscript received December 6, 2005

Accepted December 12, 2005

IE050568M